Polymer Degradation and Stability 158 (2018) 220–227

Contents lists available at ScienceDirect

Polymer Degradation and Stability

journal homepage: www.elsevier.com/locate/polydegstab

Effects of heat treatment on the chemical compositions and thermal decomposition kinetics of Japanese cedar and beech wood

Yi-Chi Chien [1], Teng-Chun Yang [1], Ke-Chang Hung, Cheng-Chun Li, Jin-Wei Xu, Jyh-Horng Wu*

Department of Forestry, National Chung Hsing University, Taichung, 402, Taiwan

ARTICLE INFO

Article history:
Received 20 August 2018
Received in revised form
25 October 2018
Accepted 4 November 2018
Available online 8 November 2018

Keywords:
Chemical composition
Heat treatment
Principal component analysis
Thermal decomposition kinetics
Wood

ABSTRACT

This study investigated variations in the chemical compositions and thermal decomposition kinetics of Japanese cedar and beech wood during heat treatment. Fourier transform infrared (FTIR) and nuclear magnetic resonance (NMR) spectra revealed that various reactions, such as hemicellulose deacetylation, condensation reactions causing lignin cross-linking, and reductions in cellulose amorphous regions, were carried out during the heat treatment process. In addition, combinations of FTIR spectra and principal component analysis (PCA) succeeded in discriminating the major changes in functional groups of wood at various heat treatment temperatures. On the other hand, the decrease in the storage modulus of wood was more rapid in the presence of oxygen than in an oxygen-free atmosphere during heat treatment. Accordingly, the activation energies of thermal decomposition using Arrhenius model for Japanese cedar and beech were 120.6 and 141.3 kJ/mol under air, respectively, while these values were 124.8 and 150.0 kJ/mol under nitrogen, respectively.

1. Introduction

Wood is a versatile, renewable, basic resource, and natural biopolymer that is widely used in different applications, and it remains indispensable to everyday human life and culture due to its aesthetic appearance and characteristic properties. In recent years, wood-based products have been developed in the wood market as the supply of large trees diminishes and the cost of wood continues to increase [1]. However, these lignocellulosic materials have a few undesirable properties, such as dimensional instability, photodegradation, combustibility, and susceptibility to biological degradation. These drawbacks have limited wood utilization in various applications. To overcome these issues, chemical approaches have been used to enhance the dimensional stability, thermal stability, photostability, and biological and weathering resistances of wood in recent decades [2–6]. However, chemical modification is costly and time-consuming and requires fastidious processing. Therefore, heat treatment, one physical modification, has attracted attention in academic and industry fields due to its cost-effectiveness and environmental friendliness.

In general, heat treatment of wood is carried out in the temperature range of 150–230 °C [7,8]. Outside of this range, the changes in wood properties are insignificant at heat treatment temperatures of less than 150 °C. Conversely, unacceptable wood degradation is observed at heat treatments temperatures greater than 260 °C [9]. Several researchers reported that heat treatment significantly improved the hygroscopic properties of a lignocellulosic material, resulting in increased dimensional stability and biological resistance due to the reduction of moisture absorption capabilities [7,10–12]. However, heat-treated wood shows the color change and exhibits a reduction in mechanical properties. Chemical changes in heat-treated wood are obviously complex because of varying amounts of cellulose, hemicellulose, lignin, and extractives in the wood cell wall. Of these components, hemicellulose is the most heat-sensitive, showing significant decomposition at 200–260 °C [13]. For chemical products of wood during heat treatment, carboxylic acids (e.g., acetic acid) are formed from cleavage of the acetyl groups in hemicelluloses [14], which are consequently hydrolyzed into oligomers and monomers [15]. On the other hand, monomeric sugar units, such as pentoses and hexoses, are dehydrated to aldehydes, such as furfural and hydroxymethylfurfural (HMF) [16]. Simultaneously, lignin undergoes depolymerization and then repolymerizes as a more

* Corresponding author.
E-mail address: eric@nchu.edu.tw (J.-H. Wu).
[1] These authors contributed equally to this work.

https://doi.org/10.1016/j.polymdegradstab.2018.11.003
0141-3910/

condensed substance with lignin-carbohydrate cross-links [10,12,17–19]. In addition, the relative amounts of crystalline cellulose are increased due to the degradation of amorphous components after heat treatment. These autocatalytic reactions of cell wall constituents, including depolymerization, dehydration, hydrolysis, oxidation, and decarboxylation, are caused by significant transformations in the chemical composition of wood.

Among various analytical methods, FTIR spectroscopy is one simple technique for rapidly obtaining information on the structural compositions of wood or modified wood [6,20–22]. However, bands cannot be directly assigned to every single component of wood, and interpretations of isolated bands can be misleading if the signal of the functional group shows poor intensity or if one single overlaps another [23,24]. Therefore, FTIR spectra with PCA was developed to characterize and analyze the complex signals in wood [25–27]. In addition, CP/MAS ^{13}C NMR has been used to characterize the changes in chemical compositions of thermally modified wood [18,28–30]. On the other hand, thermal degradation kinetics have been successfully used to describe the rates of temperature-dependent chemical reactions, and this allows prediction of the pyrolysis or degradation of lignocellulosic materials [31–35]. However, these previous studies explored thermal degradation kinetics for evaluating the changes in mechanical properties of different pieces of test samples. To the best of our knowledge, little information is available on determining changes in the viscoelastic properties of the same wood sample during heat treatment using dynamic mechanical analysis (DMA). Therefore, in addition to detailed investigations on the chemical compositions of heat-treated wood by FTIR spectra with PCA and NMR, the other objective of the present study was to investigate the time/temperature-dependent responses and thermal decomposition kinetics of heat-treated wood under different atmospheres using DMA.

2. Experimental

2.1. Preparation of heat-treated wood samples

Japanese cedar (*Cryptomeria japonica*) and beech (*Fagus sylvatica*) slicewoods were kindly provided by the experimental forest of National Chung Hsing University (Nan-Tou, Taiwan) and Ua Wood Floors Inc. (Yunlin, Taiwan), respectively. Heat-treated wood samples were exposed under a continuous flux of air or nitrogen at a flow rate of 20 mL/min with atmospheric pressure in a conventional oven (CMF-25S, Fann Chern Industrial Co., Taichung, Taiwan). Before heat treatment, the samples were first oven-dried at 105 °C for 24 h. The oven was further heated from 105 °C to the desired temperature (140, 160, 180, 200, 220, and 260 °C) at a heating rate of 10 °C/min. The heat treatments were conducted at the desired temperature for 2 h, and the samples were then cooled to room temperature in 40 min. The dimensions of the samples of heat-treated wood were 250 mm (L) × 100 mm (T), each having a thickness of 3 mm.

2.2. Solid-state CP/MAS ^{13}C NMR analysis

The samples were examined by solid state cross-polarization magic angle spin (CP/MAS) carbon 13 nuclear magnetic resonance (^{13}C NMR). The spectra were recorded on a Bruker DSX-400WB FT-NMR spectrometer (Bremen, Germany) with a sampling frequency of 100 MHz. The chemical shifts were calculated relative to tetramethylsilane (TMS). Duplicate specimens were used for each determination.

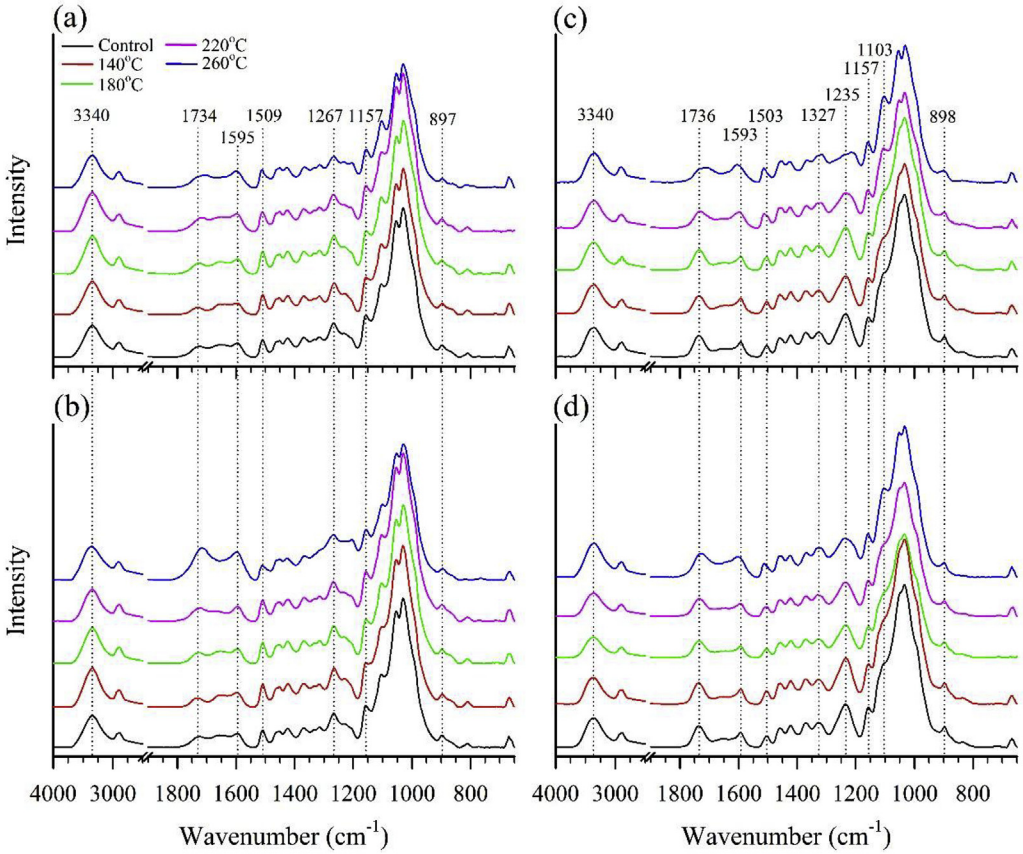

Fig. 1. FTIR spectra of wood samples as heat treatment proceeds under different atmospheres. Japanese cedar under air (a) or nitrogen (b); beech under air (c) or nitrogen (d).

Table 1
Assignments of bands in the IR spectra of untreated wood samples.

Absorption (cm^{-1})		Assignment
Japanese cedar	Beech	
3340	3340	O–H stretching
2903	2903	C–H stretching in CH_2 and CH_3
1734	1736	C=O stretching of carboxyl groups and acetyl groups in hemicellulose
1595	1593	Aromatic skeletal stretching in lignin
1509	1503	Aromatic skeletal stretching in lignin
1452	1459	C–H deformation in lignin and xylan
1424	1422	Aromatic skeletal stretching and C–H in-plane bending in lignin and carbohydrates
1370	1370	Aliphatic C–H stretching in methyl and phenol OH
–	1327	C_1–O stretching in syringyl derivatives
1316	–	CH_2 wagging in cellulose and hemicellulose
1267	–	Guaiacyl ring breathing, C=O stretching in lignin, and C–O linkage in guaiacyl aromatic methoxyl groups
1233	1235	C–C, C–O, and C=O stretching in lignin and xylan
1157	1157	C–O–C stretching in pyranose rings and C=O stretching in aliphatic groups
1030	1034	C–O deformation in primary alcohols, C=O stretching (nonconjugated), and aromatic C–H in-plane deformation
897	898	C_1–H bending in cellulose and asymmetric out-of-plane ring stretching in cellulose

2.3. ATR-FTIR spectral measurements

Fourier transform infrared (FTIR) spectra of untreated and heat-treated wood samples were recorded on a Spectrum 100 FTIR spectrometer (Perkin Elmer, Buckinghamshire, UK) equipped with a DTGS (deuterated triglycine sulfate) detector and a MIRacle attenuated total reflectance (ATR) accessory (Pike Technologies, Wisconsin, USA). The spectra were collected by co-adding 32 scans at a resolution of 4 cm^{-1} in the 650 to 4000 cm^{-1} range.

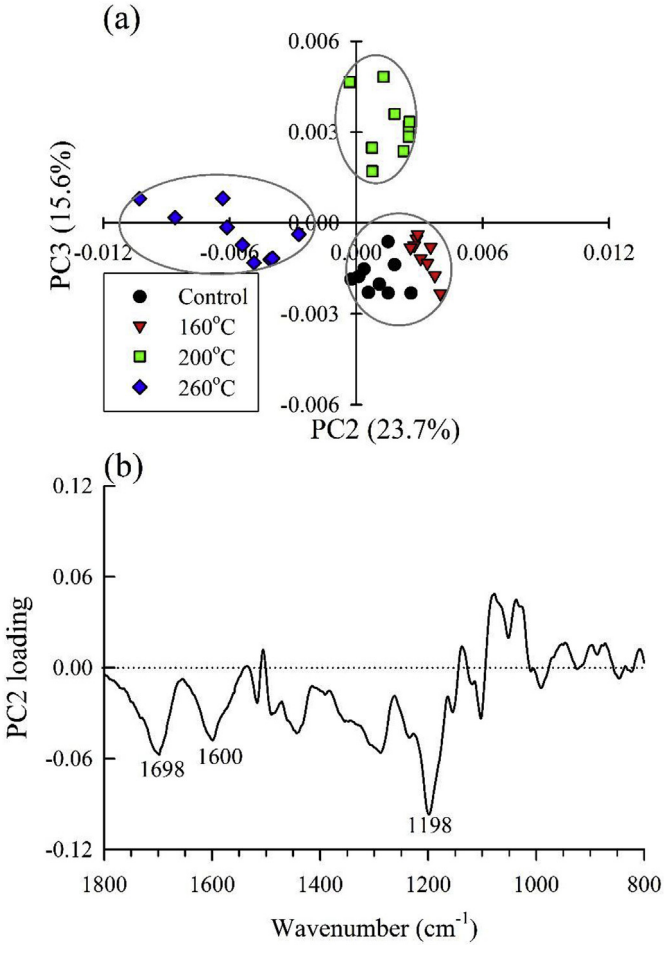

Fig. 2. PCA of second-derivative ATR-FTIR spectra for Japanese cedar as heat treatment proceeds under air. (a) Score scatter plot of PC2 versus PC3; (b) PC2 loading profile.

2.4. Principal component analysis (PCA)

FTIR spectra were statistically analyzed by PCA using MVSP version 3.1 software (Kovach Computing Services, Wales, UK). The 1800–800 cm^{-1} region of the ATR spectra was vector normalized, and the resulting data were analyzed per previously reported methods [36].

2.5. Thermal decomposition kinetics by DMA

The thermal decomposition kinetics of wood were measured in single cantilever bending mode by dynamic mechanical analysis (DMA 8000, Perkin Elmer, Buckinghamshire, UK) at a heating rate of 10 °C/min to the desired temperature at a frequency of 1 Hz. The storage modulus (E') was recorded under isothermal conditions in the 120–220 °C temperature range with an interval of 20 °C for 2 h. The dimensions of the samples were 57 mm (L) × 12 mm (T) with a thickness of 3 mm. The straight longitudinal grain, free of defects, and modulus of elasticity (MOE) ranged from 9.0 to 10.0 GPa and from 13.0 to 14.0 GPa for oven-dried Japanese cedar and beech were used, respectively. To investigate thermal decomposition kinetics, the loss of E' at each temperature over the time period was linearized to estimate the temperature-dependent decomposition rate, $\kappa(T)$, which was considered independent from the duration time and was calculated by Eq. (1). Many studies have explored decomposition rates for evaluating the changes in any measured property of lignocellulosic materials, such as color changes, mass loss, and mechanical properties [32,34,35,37–40]. Based on this kinetic theory, the first-order kinetics rates over time are presumably dependent on temperature via the Arrhenius activation energy model in Eq. (2) [41]. The model can be represented in natural logarithmic forms in Eq. (3) to obtain E_a for both wood samples at different heat treatment temperatures.

$$\frac{dE'(t,\ T)}{dt} = -\kappa(T) \tag{1}$$

$$\kappa(T) = Ae^{-E_a/RT} \tag{2}$$

$$ln\ \kappa(T)\ =\ ln\ A - \frac{E_a}{RT} \tag{3}$$

where A is constant (pre-exponential factor), E_a is the activation

energy, R is the universal gas constant (8.314 J/K/mol), and T is the absolute temperature (K).

3. Results and discussion

3.1. Characteristic bands in the FTIR spectrum

The effects of heat treatment temperatures under different atmospheres on the chemical compositions of Japanese cedar and beech were characterized by ATR-FTIR, as shown in Fig. 1. Assignments and peak positions of untreated wood samples are listed in Table 1 [20,22,26,42,43]. To compare the spectra of untreated and heat-treated samples, all spectra were normalized to the C–H aliphatic stretching peak at 2903 cm^{-1} [21]. First, the bands at 1734 (Japanese cedar) and 1736 (beech) cm^{-1} were assigned to the stretching of the carbonyl groups of acetyls in hemicellulose. As expected, this specific acetyl absorption band was obviously stronger in beech than in Japanese cedar. Under air, however, the band intensities of both wood samples decreased with increasing heat treatment temperatures. This result indicates that heat treatment causes deacetylation of hemicellulose by the cleavage of acetyl groups [10,12]. When wood was heat-treated under nitrogen, the band intensities slightly decreased with increasing heat treatment temperatures up to 220 °C. Once the heat treatment temperature reached 260 °C, a significant increase in carbonyl bands was observed, and they shifted to lower wavenumbers. This result can be explained by the fact that attendant acids (e.g., formic acid) react with hydroxyl groups to form new carbonyl groups by esterification reactions. A similar result was reported by several researchers [43,44].

On the other hand, bands of aromatic skeletal stretching in lignin appeared at 1595 and 1593 cm^{-1} for Japanese cedar and beech, respectively. The intensities of these bands increased with increasing heat treatment temperatures. Compared to the air treatment, dramatic changes in the intensities of these bands were observed for both wood samples at 260 °C under nitrogen treatment (Fig. 1b and d). An increase in the intensities of these bands was attributed to the fact that the relative percentage of lignin increased due to polysaccharide degradation, especially hemicellulose degradation. In addition, the previous study revealed that splitting the aliphatic side chains in lignin and condensation reactions of lignin caused cross-link formations [45,46]. This phenomenon can cause a reduction in water absorption, further decreasing the shrinking and swelling of wood [19]. The other characteristic band of aromatic ring stretching appeared at approximately 1500 cm^{-1}, and the bands at 1509 and 1503 cm^{-1} corresponded to guaiacyl-type and guaiacyl/syringyl-type lignins for softwood (Japanese cedar) and hardwood (beech), respectively [22,47]. These band intensities increased with an increase in thermal temperatures up to 220 °C and then decreased at 260 °C. Additionally, the band for beech shifted to a higher wavenumber when it was heat-treated at 260 °C. The results can be explained by the fact that the syringyl moiety of lignin thermally decomposes more rapidly than the guaicyl moiety [22,48].

In addition, the band corresponding to C–O stretching at 1103 cm^{-1} appeared to be significant for beech at heat treatments above 220 °C. This might have been due to the formation of an ether linkage from the hydroxyl groups within hemicelluloses and lignin [45] or to the formation of new alcohols and esters [21] during heat treatment. Furthermore, after heat treatment, we noted a slight reduction in the asymmetric ring stretching band of cellulose at 897 and 898 cm^{-1} for Japanese cedar and beech wood, respectively. This result implies that soluble acidic constitutions (e.g., formic acid, acetic acid, etc.) from the hemicellulose degradation caused depolymerization of cellulose by breaking down long chains to shorter chains.

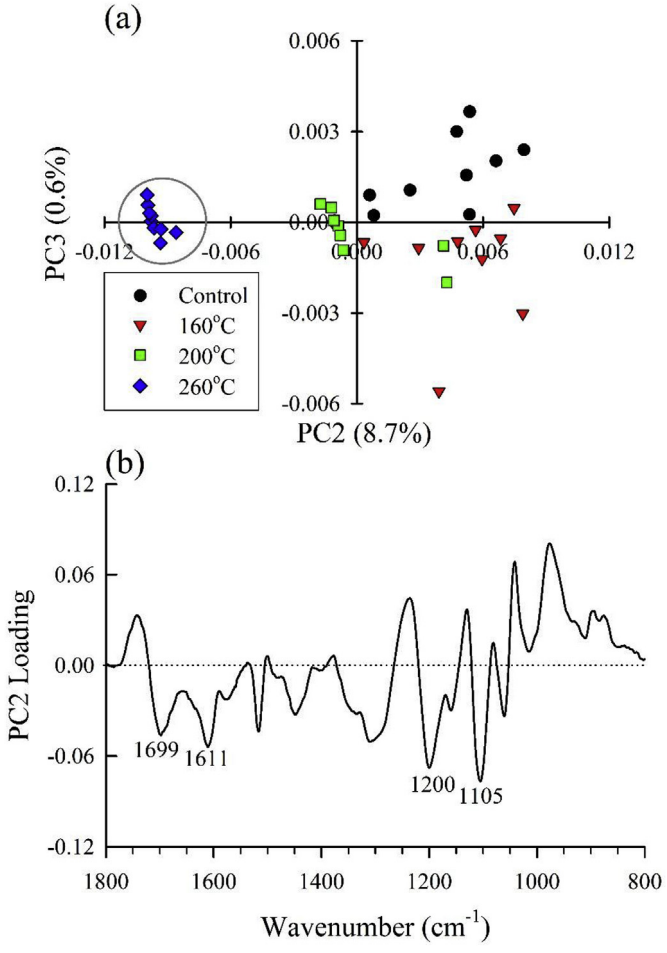

Fig. 3. PCA of second-derivative ATR-FTIR spectra for beech as heat treatment proceeds under air. (a) Score scatter plot of PC2 versus PC3; (b) PC2 loading profile.

3.2. ATR-FTIR spectroscopy combined with PCA

In the previous section, functional groups of Japanese cedar and beech during heat treatment under air and nitrogen were investigated. To obtain more information on temperature-dependent differences in all wood samples, ATR-FTIR spectroscopy with PCA was conducted. From the results of FTIR spectra, similar major changes in functional groups of all samples were observed regardless of treatment with air or with nitrogen. Therefore, this section outlines using PCA to distinguish differences in the chemical components of wood during heat treatments at 160, 200, and 260 °C under air. In addition, the spectra were converted into second derivatives due to several advantages: the influence of baseline shifts is diminished, and thus, the reproducibility of spectra is elevated [49]; and typical spectral features are easier to discriminate [26,50,51].

A mean-centered PCA was conducted based on the second-derivative ATR-FTIR spectra of all samples over the 1800–800 cm^{-1} range (fingerprint region), which is dominated by stretching vibrations of C=C, C=O, C–O, ring structures, and deformation vibrations of CH_2 groups [42,50,52,53]. This region was found to be useful for polysaccharide identification [25–27]. Fig. 2a shows the score scatter plot of PC2 versus PC3 for Japanese cedar at different temperatures under air treatment. The results accounted for 39.3% of the total variability, with PC2 and PC3

accounting for 23.7% and 15.6%, respectively. Distinct segregation and clustering was apparent between Japanese cedar at different treatment temperatures, and a robust separation was easily achieved by combining PC2 with PC3. Remarkably, three groups could be observed based on the score scatter plot: one for untreated and heat-treated samples at 160 °C, another for heat-treated samples at 200 °C, and a third for heat-treated samples at 260 °C, with scores located on the negative side of PC2. These differentiations most likely reflect the main changes in the functional groups of Japanese cedar when it was heat-treated above 200 °C. Furthermore, loading plots were generated to highlight the contribution of each variable (wavenumber) to each principal component [49]. As shown in Fig. 2b, PC2 loadings may be used to interpret sample separations of heat-treatments at 260 °C, as their scores were negative in the PC2 axis. The major contributors to spectral variation were at 1698, 1600, and 1198 cm^{-1}. At 1698 cm^{-1}, the absorption of carbonyl groups (C=O) of aldehydes, such as furfural and HMF, which act as cross-linkers between two aromatic rings [54], were visible. Brebu et al. [55] reported that this absorption can also result from pyrolysis products of lignin, such as vanillin. In addition, the band at 1600 cm^{-1} corresponded to the degree of condensation of lignin fractions [54]. Finally, the band at 1198 cm^{-1} could be assigned to ether linkages (C–O–C) from crosslinks by the thermal degradation of lignin or to products of the thermal degradation of cellulose and hemicellulose [56].

On the other hand, Fig. 3a shows the score scatter plot of PCA for beech at different temperatures under air treatment. PC2 and PC3 accounted for 9.3% of the total variability (8.7 and 0.3%, respectively). Only beech that was treated at 260 °C exhibited distinct segregation and clustering from the other groups. In the PC2 loadings profile of untreated and heat-treated beech (Fig. 3b), we observed negative loadings at 1699, 1611, and 1200 cm^{-1}, which were similar to the PC2 loadings profile for Japanese cedar. Additionally, a major negative absorbance at 1105 cm^{-1} was attributed to the formation of new C–O groups during heat treatment, as mentioned previously.

3.3. Characteristics in the NMR spectrum

Solid-state CP/MAS ^{13}C NMR was used to elucidate the characteristics of untreated and heat-treated samples. As shown in Figs. 4 and 5, both untreated Japanese cedar and beech wood showed typical lignocellulosic characteristics. Cellulose appeared in the 60–105 ppm region. The signal at 105.0 ppm was attributed to C1

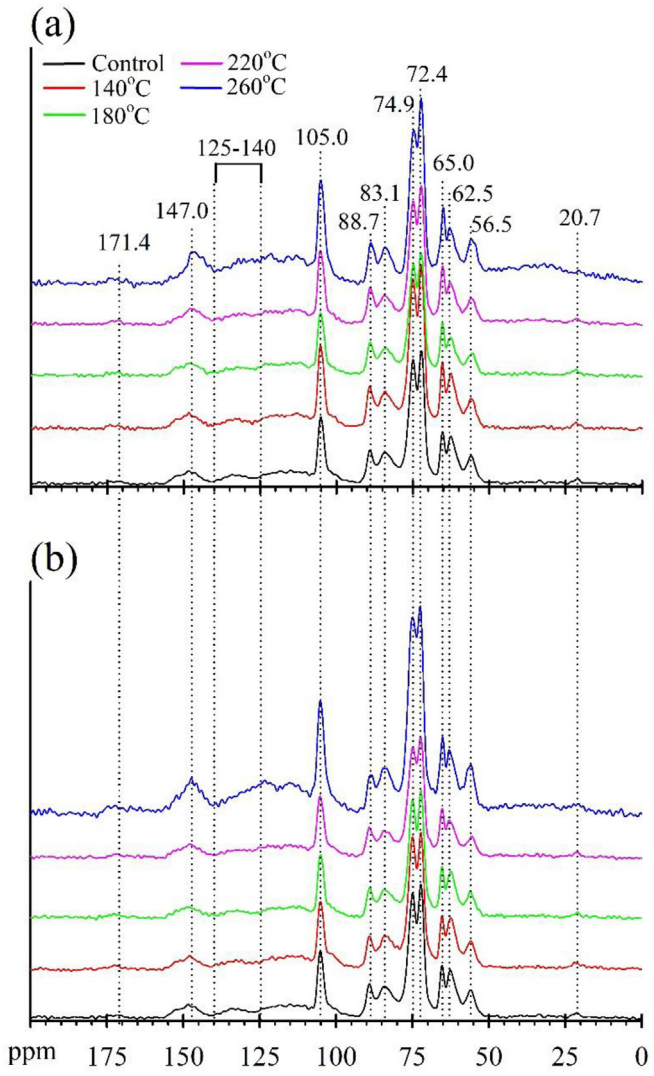

Fig. 4. ^{13}C CP/MAS NMR spectra of Japanese cedar as heat treatment proceeds under different atmospheres. (a) Air; (b) nitrogen.

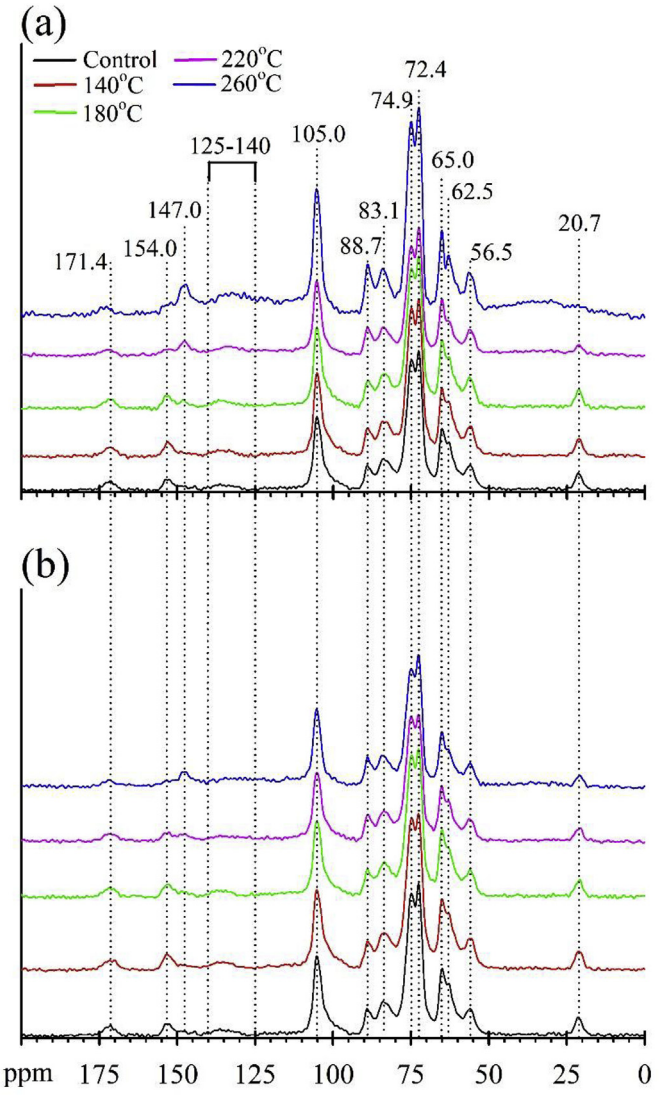

Fig. 5. ^{13}C CP/MAS NMR spectra of beech as heat treatment proceeds under different atmospheres. (a) Air; (b) nitrogen.

anomeric carbon. Signals at 88.7 and 83.1 ppm were assigned to the C4 of crystalline and amorphous cellulose, respectively [57,58]. Signals at 74.9 and 72.4 ppm were ascribed to the C2 and C3, C5 carbons of cellulose, while 65.0 and 62.5 ppm corresponded to the C6 of ordered and disordered cellulose. Signals of hemicellulose carbons could not be precisely identified due to exhibiting an overlapping field with cellulose carbons [59,60]. Therefore, the signals at 171.4 and 20.7 ppm were for hemicellulose and were assigned to the carboxylic (CH_3COO-) and methyl (CH_3COO-) carbons of acetyl groups. Beech signals were more obvious than Japanese cedar signals due to higher hemicellulose content, especially the acetylated xylans content. After heat treatment, the signals at 171.4 and 20.7 ppm for all samples decreased with increasing temperature, especially under air treatment (Figs. 4a and 5a). Due to the higher content of acetyl groups in untreated beech, the reduction in hemicellulose deacetylation was clearly more pronounced in beech than in Japanese cedar. In addition, with an increase in heat treatment temperature, the signal at 147 ppm increased for Japanese cedar, while shifting of the signal at 154 ppm in untreated beech to 147 ppm in heat-treated beech was clearly observed. These results indicate modifications in aryl–ether structures of the lignin network. On the other hand, a broadened signal between 125 and 140 ppm appeared for all samples after heat treatment at temperatures greater than 220 °C except for beech wood under nitrogen treatment. This is ascribable to the thermal cross-linking of lignin [18,30,54,61]. Furthermore, compared to the signal at 65.0 ppm (crystalline C6), the intensities of signals at 62.5 ppm (amorphous C6) significantly decreased above 220 °C, indicating an increase in the crystallinity of the wood. Wood crystallinity is well known to increase with heat treatment due to preferential degradation of the disordered molecules of amorphous cellulose and hemicelluloses [19]. In addition, this phenomenon at different temperatures was more obvious under air treatment than under nitrogen treatment. According to the NMR spectra in this study, the main changes in the chemical compositions of all samples during heat treatment were (1) deacetylation of hemicellulose, (2) increased thermal cross-linking of lignin, and (3) increased crystallinity of cellulose. Moreover, these signals were dramatically altered for both wood samples under air treatment compared to those under nitrogen treatment.

3.4. Thermal decomposition kinetics

To investigate thermal decomposition kinetics, DMA was used to estimate the change in storage modulus (E') of wood during the thermal degradation process. Fig. 6 shows the E' duration curves of Japanese cedar and beech under air and nitrogen atmospheres at various isothermal conditions. The initial E' values of all samples decreased as the heat treatment temperatures increased. For instance, when wood samples were heat-treated from 120 °C to 220 °C under air, the initial E' decreased from 3.8 GPa to 1.2 GPa (decreased by 68%) and from 4.8 GPa to 3.4 GPa (decreased by 29%) for Japanese cedar and beech, respectively (Fig. 6a and c). Little change was observed in E' as a function of time at lower temperatures (below 140 °C), whereas a slow decline was observed in the 160–180 °C range. When the temperature exceeded 200 °C, dramatic change in E' were obvious. These phenomena agreed with the ATR-FTIR spectroscopy and NMR results in this study. The major factor underlying these results is the deacetylation of hemicelluloses. Released acetic acid acts as a depolymerization catalyst that further increases polysaccharide decomposition [17,28,29,62], causing loss of mass, density, and mechanical properties [8,63]. The

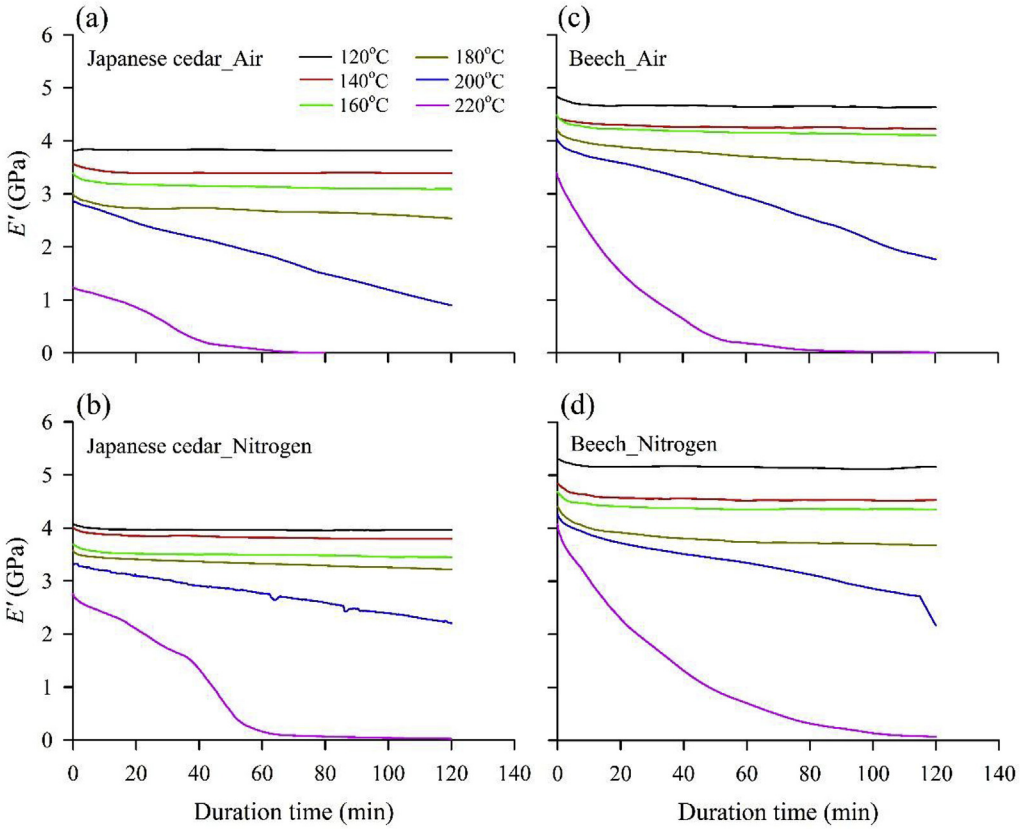

Fig. 6. Duration curves of the storage modulus (E') of wood samples under different isothermal conditions. Japanese cedar under air (a) or nitrogen (b); beech under air (c) or nitrogen (d).

oxidative degradation of both wood samples was clearly observable as time increased at sufficient temperatures regardless of treatment in air or the nitrogen purge. However, the decrease in E' was more dramatic under air than under nitrogen. For example, for Japanese cedar at 200 °C after 2 h, the E' was reduced by 69% under air and by 33% under nitrogen (Fig. 6a and b). These results demonstrate that thermal decomposition for heat-treated wood was more rapid in the presence of oxygen than in an oxygen-free atmosphere. This tendency was similar to the report by Kubojima et al. [64]. On the other hand, the decomposition rate of beech was higher than that of Japanese cedar due to the higher content of acetyl groups in the cell walls of beech [23].

To further investigate the thermal decomposition kinetics of wood under different atmospheres, the E' values at all exposure temperatures over time were fit to straight lines based on an assumption of a constant. In this study, the decomposition rate, $\kappa(T)$, found the slopes of linear fit in the 160–220 °C range to avoid obtaining a negative degradation rate. As shown in Fig. 7, the decomposition rate on a natural log scale versus the inverse of the absolute temperature (T) was plotted. Activation energy (E_a) can be calculated from the slope of the plot of $\ln(\kappa)$ versus $1/T$. A linear regression was performed on the slope, and the R^2 values of all wood samples were greater than 0.97, suggesting that the change in E' during heat treatment can be explained as first-order thermal decomposition kinetics. Accordingly, the E_a values for Japanese cedar were 120.6 kJ/mol and 124.8 kJ/mol under air and nitrogen, respectively, whereas those for beech were 141.3 kJ/mol and 150.0 kJ/mol under air and nitrogen, respectively. This result reveals that heat treating woods requires more activation energy under nitrogen than under air. Additionally, the E_a value of beech was higher than that of Japanese cedar due to the higher hemicellulose contents for beech. For thermal decomposition kinetics, several researchers calculated activation energy of heat-treated wood from color changes, mass loss, and reduction in mechanical properties. Matsuo et al. [34] calculated the activation energy of heat-treated wood under air from color changes in the 95–117 kJ/mol range. On the other hand, the E_a value of heat-treated wood from mass loss under air and nitrogen presented as 71 kJ/mol and 155 kJ/mol, respectively [32]. According to the reduction in mechanical properties, the E_a value of heat-treated wood under air was calculated to be 74–130 kJ/mol [31,33]. These activation energies were similar to those in the present study that analyzed the loss of E' by isothermal DMA.

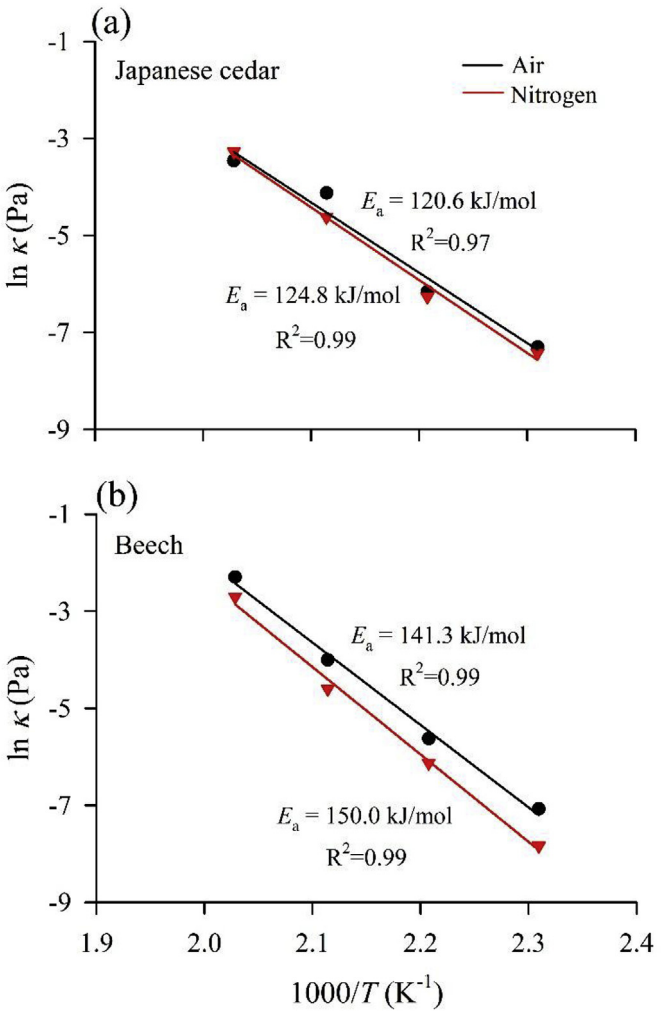

Fig. 7. Correlation between the natural log of the degradation rate (κ) and reciprocal absolute temperature of wood samples. Japanese cedar (a); beech (b).

4. Conclusions

The chemical compositions and thermal decomposition rates of wood were substantially influenced by the temperature and treatment atmosphere. Deacetylation of hemicellulose, cross-linking of lignin caused by condensation reactions, and reduction in amorphous regions of cellulose were observed from FTIR and NMR spectra analyses of heat-treated wood samples, particularly in the presence of oxygen and treatment temperatures above 220 °C. In addition, FTIR spectra combined with PCA showed distinct segregation and clustering for Japanese cedar that was treated at different temperatures under air. However, only beech that was treated at 260 °C was segregated and clustered. Based on loading PCA plots, the major contributors to spectral variations of heat-treated wood samples were determined to be the carbonyl groups from aldehyde formation and ether linkages from crosslinks of thermally degraded lignin or pyrolysis products of cellulose and hemicellulose. Furthermore, according to the variation in the storage modulus (E') as a function of time, the E' loss rate of beech was higher than that of Japanese cedar due to higher acetyl group contents in the cell walls of beech. In addition, the thermal decomposition of heat-treated wood was more rapid under air than under nitrogen. On the other hand, the activation energy (E_a) was successfully calculated by first-order thermal decomposition kinetics from the loss of E'. The results revealed that heat treating wood required more activation energy under nitrogen than under air. Consequently, these results not only provide information regarding changes in the chemical compositions of wood but also offer feasibility for evaluating the thermal decomposition kinetics of wood using isothermal DMA tests.

Acknowledgements

This work was financially supported by a research grant from the Ministry of Science and Technology in Taiwan (NSC 102-2628-B-005-006-MY3).

References

[1] R.B. Hoadley (Ed.), Understanding Wood: a Craftsman's Guide to Wood Technology, The Taunton Press, Newtown, 2000.
[2] J.H. Wu, T.Y. Hsieh, H.Y. Lin, I.L. Shiau, S.T. Chang, Properties of wood plasticization with octanoyl chloride in a solvent-free system, Wood Sci. Technol. 37 (2004) 363–372.
[3] R.W. Rowell, Chemical modification of wood: a short review, Wood Mater. Sci. Eng. 1 (2006) 29–33.
[4] P.D. Evans, Review of the weathering and photostability of modified wood, Wood Mater. Sci. Eng. 4 (2009) 2–13.

[5] K.C. Hung, J.H. Wu, Mechanical and interfacial properties of plastic composite panels made from esterified bamboo particles, J. Wood Sci. 56 (2010) 216–221.
[6] C.N. Yang, K.C. Hung, T.L. Wu, T.C. Yang, Y.L. Chen, J.H. Wu, Comparisons and characteristics of slicewood acetylation with acetic anhydride by liquid phase, microwave, and vapor phase reactions, BioResources 9 (2014) 6463–6475.
[7] G. Gündüz, S. Korkut, D.S. Korkut, The effects of heat treatment on physical and technological properties and surface roughness of Camiyani Black Pine (*Pinus nigra* Arn. subsp. *pallasiana* var. *pallasiana*) wood, Bioresour. Technol. 99 (2008) 2275–2280.
[8] S. Korkut, M.S. Kök, D.S. Korkut, T. Gürleyen, The effects of heat treatment on technological properties in Red-bud maple (*Acer trautvetteri* Medw.) wood, Bioresour. Technol. 99 (2008) 1538–1543.
[9] C.A.S. Hill (Ed.), Wood Modification: Chemical, Thermal and Other Processes, John Wiley & Sons, West Sussex, 2006.
[10] M. Altgen, T. Uimonen, L. Rautkari, The effect of de- and re-polymerization udring heat-treatment on the mechanical behavior of Scots pine sapwood under quasi-static load, Polym. Degrad. Stabil. 147 (2018) 197–205.
[11] P. Bekhta, P. Niemz, Effect of high temperature on the change in color, dimensional stability and mechanical properties of spruce wood, Holzforschung 57 (2003) 539–546.
[12] M. Altgen, W. Willems, R. Hosseinpourpia, L. Rautkari, Hydroxyl accessibility and dimensional changes of Scots pine sapwood affected by alterations in the cell wall ultrastructure during heat-treatment, Polym. Degrad. Stabil. 152 (2018) 244–252.
[13] D. Mohan, C.U. Pittman, P.H. Steele, Pyrolysis of wood/biomass for bio-oil: a critical review, Energy Fuel. 20 (2006) 848–889.
[14] J. Bourgois, R. Guyonnet, Characterization and analysis of torrefied wood, Wood Sci. Technol. 22 (1988) 143–155.
[15] F. Carrasco, C. Roy, Kinetic study of dilute-acid prehydrolysis of xylan-containing biomass, Wood Sci. Technol. 26 (1992) 189–208.
[16] E. Burtscher, O. Bobleter, W. Schwald, R. Concin, H. Binder, Chromatographic analysis of biomass reaction products produced by hydrothermolysis of poplar wood, J Chromatoger A 390 (1987) 401–412.
[17] M. Nuopponen, T. Vuorinen, S. Jämsä, P. Viitaniemi, Thermal modifications in softwood studied by FT-IR and UV resonance Raman spectroscopies, J. Wood Chem. Technol. 24 (2005) 13–16.
[18] M. Hakkou, M. Pétrissans, A. Zoulalian, P. Gérardin, Investigation of wood wettability changes during heat treatment on the basis of chemical analysis, Polym. Degrad. Stabil. 89 (2005) 1–5.
[19] M.J. Boonstra, B.F. Tjeerdsma, Chemical analysis of heat-treated softwoods, Holz Roh Werkst 64 (2006) 204–211.
[20] C.M. Popescu, C. Vasile, M.C. Popescu, G. Singurel, Degradation of lime wood painting supports II. Spectral characterization, Cellul. Chem. Technol. 40 (2006) 649–658.
[21] D. Kocaefe, S. Poncsak, Y. Boluk, Effect of thermal treatment on the chemical composition and mechanical properties of birch and aspen, BioResources 3 (2008) 517–537.
[22] B. Esteves, A.V. Marques, I. Domingos, H. Pereira, Chemical changes of heat treated pine and eucalypt wood monitored by FTIR, Maderas Cienc. Technol. 15 (2013) 245–258.
[23] A.J. Michell, Infra-red spectroscopy transformed – new applications in wood and pulping chemistry, Appita J. 41 (1988) 375–380.
[24] N.L. Owen, D.W. Thomas, Infrared studies of “hard” and “soft” woods, Appl. Spectrosc. 43 (1989) 451–455.
[25] R. Hori, J. Sugiyama, A combined FT-IR microscopy and principal component analysis on softwood cell walls, Carbohydr. Polym. 52 (2003) 449–453.
[26] H. Chen, C. Ferrai, M. Angiuli, J. Yao, C. Raspi, E. Bramanti, Qualitative and quantitative analysis of wood samples by Fourier transform infrared spectroscopy and multivariate analysis, Carbohydr. Polym. 82 (2010) 772–778.
[27] R. Rana, R. Langenfeld-Heyser, R. Finkeldey, A. Polle, FTIR spectroscopy, chemical and histochemical characterisation of wood and lignin of five tropical timber wood species of the family of Dipterocarpaceae, Wood Sci. Technol. 44 (2010) 225–242.
[28] B.F. Tjeerdsma, M. Boonstra, A. Pizzi, P. Tekely, H. Militz, Characterisation of thermally modified wood: molecular reasons for wood performance improvement, Holz Roh Werkst 56 (1998) 149–153.
[29] H. Sivonen, S.L. Maunu, F. Sundholm, S. Jämsä, P. Viitaniemi, Magnetic resonance studies of thermally modified wood, Holzforschung 56 (2002) 648–654.
[30] H. Wikberg, S.L. Maunu, Characterisation of thermally modified hard- and softwoods by ^{13}C CPMAS NMR, Carbohydr. Polym. 58 (2004) 461–466.
[31] A.J. Stamm, Thermal degradation of wood and cellulose, Ind. Eng. Chem. 48 (1956) 413–417.
[32] F. Shafizadeh, A.G.W. Bradbury, Thermal degradation of cellulose in air and nitrogen at low temperatures, J. Appl. Polym. Sci. 23 (1979) 1431–1442.
[33] M. Gao, C.Y. Sun, C.X. Wang, Thermal degradation of wood treated with flame retardants, J. Therm. Anal. Calorim. 85 (2006) 765–769.
[34] M. Matsuo, M. Yokoyama, K. Umemura, J. Gril, K. Yano, S. Kawai, Color changes in wood during heating: kinetic analysis by applying a time-temperature superposition method, Appl. Phys. A 99 (2010) 47–52.
[35] A. Sinha, J.A. Nairn, R. Gupta, Thermal degradation of bending strength of plywood and oriented strand board: a kinetics approach, Wood Sci. Technol. 45 (2011) 315–330.
[36] C.H. Lee, T.L. Wu, Y.L. Chen, J.H. Wu, Characteristics and discrimination of five types of wood-plastic composites by FTIR spectroscopy combined with principal component analysis, Holzforschung 64 (2010) 699–704.
[37] M. Matsuo, K. Umemura, S. Kawai, Kinetic analysis of color changes in keyaki (*Zelkova serrata*) and sugi (*Cryptomeria japonica*) wood during heat treatment, J. Wood Sci. 60 (2014) 12–20.
[38] M. Matsuo, M. Yokoyama, K. Umemura, J. Sugiyama, S. Kawai, J. Gril, S. Kubodera, T. Mitsutani, H. Ozaki, M. Sakamoto, M. Imamura, Ageing of wood: analysis of color changes during natural aging and heat treatment, Holzforschung 65 (2011) 361–368.
[39] T. Inagaki, Y. Asanuma, S. Tsuchikawa, Selective assessment of duplex heat-treated wood by near-infrared spectroscopy with principle component and kinetic analysis, J. Wood Sci. 64 (2018) 6–15.
[40] M. Polette, A.J. Zattera, R.M.C. Santana, Thermal decomposition of wood: kinetics and degradation mechanisms, Bioresour. Technol. 126 (2012) 7–12.
[41] J.E. Winandy, P.K. Lebow, Kinetics models for thermal degradation of strength of fire-retardant-treated wood, Wood Fiber Sci. 28 (1996) 39–52.
[42] E. Adler, Lignin chemistry–past, present and future, Wood Sci. Technol. 11 (1977) 169–218.
[43] D. Fengel, X. Shao, Studies on the lignin of the bamboo species *Phyllostachys makinoi* Hay, Wood Sci. Technol. 19 (1985) 131–137.
[44] B.F. Tjeerdsma, H. Militz, Chemical changes in hydrothermal treated wood: FTIR analysis of combined hydrothermal and dry heat-treated wood, Holz Roh Werkst 63 (2005) 102–111.
[45] X. Colom, F. Carrillo, F. Nogués, P. Gaariga, Structural analysis of photo-degraded wood by means of FTIR spectroscopy, Polym. Degrad. Stabil. 80 (2003) 543–549.
[46] D. Erçin, Y. Yürüm, Carbonization of Fir (*Abies bornmulleriana)* wood in an open pyrolysis system at 50–300°C, J. Anal. Appl. Pyrol. 67 (2003) 11–22.
[47] O. Faix, Classification of lignins from different botanical origins by FT-IR spectroscopy, Holzforschung 45 (1991) 21–27.
[48] O. Faix, D. Meier, I. Fortmann, Thermal degradation products of wood. Gas chromatographic separation and mass spectrometric characterization of monomeric lignin derived products, Holz Roh Werkst. 48 (1990) 281–285.
[49] M. Kansiz, P. Heraud, B. Wood, F. Burden, J. Beardall, D. McNaughton, Fourier transform infrared microspectroscopy and chemometrics as a tool for the discrimination of cyanobacterial strains, Phytochemistry 52 (1999) 407–417.
[50] M. Tsuboi, Infrared spectrum and crystal structure of cellulose, J. Polym. Sci. 25 (1957) 159–171.
[51] C. Sandt, G.D. Sockalingum, D. Aubert, H. Lepan, C. Lepouse, M. Jaussaud, A. Leon, J.M. Pinon, M. Manfait, D. Toubas, Use of Fourier-transform infrared spectroscopy for typing of *Candida albicans* strains isolated in intensive care units, J. Clin. Microbiol. 41 (2003) 954–959.
[52] C.Y. Liang, R.H. Marchessault, Infrared spectra of crystalline polysaccharides. I. Hydrogen bonds in native celluloses, J. Polym. Sci. 37 (1959) 385–395.
[53] K.M. Dokken, L.C. Davis, N.S. Marinkovic, Use of infrared microspectroscopy in plant growth and development, Appl. Spectrosc. Rev. 40 (2005) 301–326.
[54] N. Brosse, R.E. Hage, M. Chaouch, M. Pétrissans, S. Dumarçay, P. Gérardin, Investigation of the chemical modifications of beech wood lignin during heat treatment, Polym. Degrad. Stabil. 95 (2010) 1721–1726.
[55] M. Brebu, C. Vasile, Thermal degradation of lignin–a review, Cellul. Chem. Technol. 44 (2010) 353–363.
[56] R. Singh, S. Singh, K.D. Trimukhe, K.V. Pandare, K.B. Bastawade, D.V. Gokhale, A.J. Varma, Lignin–carbohydrate complexes from sugarcane bagasse: preparation, purification, and characterization, Carbohydr. Polym. 62 (2005) 57–66.
[57] D.L. VanderHart, R.H. Atalla, Studies of microstructures in native celluloses using solid-state ^{13}C NMR, Macromolecules 17 (1984) 1465–1472.
[58] R.H. Atalla, D.L. VanderHart, The role of solid state 13C NMR spectroscopy in studies of the nature of native celluloses, Solid State Nucl. Magn. Reson. 15 (1999) 1–19.
[59] J.F. Haw, G.E. Maciel, C.J. Biermann, Carbon-13 nuclear magnetic resonance study of the rapid steam hydrolysis of red oak, Holzforschung 38 (1984) 327–331.
[60] G.E. Hawkes, C.Z. Smith, J.H.P. Utley, R.R. Vargas, H. Viertler, A comparison of solution and solid state ^{13}C NMR spectra of lignins and lignin model compounds, Holzforschung 47 (1993) 302–312.
[61] G.N. Inari, S. Mounguengui, S. Dumarçay, M. Pétrissans, P. Gérardin, Evidence of char formation during wood heat treatment by mild pyrolysis, Polym. Degrad. Stabil. 92 (2007) 997–1002.
[62] B. Esteves, H. Pereira, Wood modification by heat treatment: a review, BioResources 4 (2009) 370–404.
[63] B. Esteves, A.V. Marques, I. Domingos, H. Pereira, Influence of steam heating on the properties of pine (*Pinus pinaster*) and eucalypt (*Eucalyptus globulus*) wood, Wood Sci. Technol. 41 (2007) 193–207.
[64] Y. Kubojima, T. Okano, M. Ohta, Bending strength and toughness of heat-treated wood, J. Wood Sci. 46 (2000) 8–15.